Theory and examples of the inverse Frobenius–Perron problem for complete chaotic maps

Article *in* Chaos · July 1999

DOI: 10.1063/1.166413 · Source: PubMed

3 authors, including:

Peter Schmelcher
Hamburg University
797 PUBLICATIONS **13,961** CITATIONS

SEE PROFILE

F. K. Diakonos
National and Kapodistrian University of Athens
308 PUBLICATIONS **4,639** CITATIONS

SEE PROFILE

Theory and examples of the inverse Frobenius–Perron problem for complete chaotic maps

D. Pingel and P. Schmelcher
Theoretische Chemie, Physikalisch-Chemisches Institut, Universität Heidelberg, Im Neuenheimer Feld 253, D-69120 Heidelberg, Germany

F. K. Diakonos
Department of Physics, University of Athens, GR-15771 Athens, Greece

(Received 16 July 1998; accepted for publication 27 January 1999)

The general solution of the inverse Frobenius–Perron problem considering the construction of a fully chaotic dynamical system with given invariant density is obtained for the class of one-dimensional unimodal complete chaotic maps. Some interesting connections between this general solution and the special approach via conjugation transformations are illuminated. The developed method is applied to obtain a class of maps having as invariant density the two-parametric beta-probability density function. Varying the parameters of the density a rich variety of dynamics is observed. Observables like autocorrelation functions, power spectra, and Liapunov exponents are calculated for representatives of this family of maps and some theoretical predictions concerning the decay of correlations are tested. © *1999 American Institute of Physics.* [S1054-1500(99)01702-4]

The construction of a one-dimensional dynamical law that generates fully chaotic dynamics obeying a given invariant density is a problem of immediate relevance in both experimental and theoretical respects. This work presents a method to systematically describe the variety of solutions to this problem. The latter is achieved by integration of the Frobenius–Perron equation with the help of an auxiliary function determining the symmetry properties of the resulting dynamical law. Variation of this function allows one to obtain in an explicit form all possible maps which have the given invariant measure in common. Our concept is applied to a class of maps possessing two-parametric power law distributions as invariant densities. Some important quantities describing the dynamics of these maps are calculated numerically, e.g., Liapunov exponents and autocorrelation functions. Other properties of the maps like the local behavior at certain critical points are investigated analytically. These characteristic values and functions show extensive variation, depending on the parameters of their invariant densities.

I. INTRODUCTION

One-dimensional iterative maps represent a very useful tool to understand the physics of complex nonlinear systems. In particular they can be used to investigate the different routes of nonlinear dynamical systems from regular to chaotic behavior[1–3] to simulate physical systems showing anomalous diffusion[4] or to analyze the underlying dynamics in time series with $1/f$ noise in their power spectrum.[5,6] In many cases and in particular from an experimental point of view the only information available for a physical system is its statistical properties (ergodic measure or time correlation function) and one is asked to design a consistent dynamical law. In a recent paper[7] we examined the possibility to construct a one-dimensional discrete dynamical system with a given invariant density. This is the so-called inverse Frobenius–Perron problem (IFPP).[8–13]

It could be shown using certain symmetry requirements that this problem possesses a unique solution. We applied our method to calculate numerically the symmetric unimodal maps with the invariant density given by the symmetric beta distribution. However the solution presented in Ref. 7 is a partial and very specialized one. Depending on the chosen symmetry constraints we can get an infinite number of such solutions. In the present paper we go one step further and present the general solution to the IFPP within the class of continuous unimodal maps for which each branch of the map covers the complete unit interval. A central role is hereby played by the function h_f which parametrizes the space of the solutions. This solution enables us to explore in depth the connection between the dynamics and statistics in one-dimensional systems. Our examples of investigation concentrate on the important family of the beta distributions. The IFPP is solved for the asymmetric case when the two exponents in the expression for the density are unequal (other properties of beta distributions have been investigated in Ref. 14). From the general solution we obtain two special solutions using two different forms for the function h_f. We then calculate the time-correlation functions and the power spectra of the corresponding dynamical systems. The question of the dependence of the statistical characteristics (singularities of the density, long time behavior of the autocorrelation function) of these systems on their dynamical characteristics (critical points) is addressed. Next we compare for a given density the dependence of the statistical properties on the form of the function h_f. A large variety of the statistical and dynamical behavior is obtained. Some theoretical predictions

concerning the asymptotic decay of the correlations or the value of the Liapunov exponents[15–18] in fully chaotic dynamical systems can be tested within the class of our examples.

The paper is organized as follows: In Sec. II we present the general solution to the IFPP for the special class of maps considered. In Sec. III we derive from the general solution of Sec. II a wide family of unimodal maps having as invariant density the beta distribution. This family of maps corresponds to two special solutions of the problem: the symmetric beta map and the special asymmetric beta map. In Sec. IV we discuss the main characteristics of the maps belonging to the beta family and we study the rich dynamical behavior which they provide. In Sec. V we calculate the autocorrelation function, the power spectrum, and the Liapunov exponent for representative members of the beta family. A connection between the dynamics and the asymptotic decay of correlations is established. Some theoretical models explaining this behavior are tested. Finally Sec. VI contains the conclusions and gives a brief outlook with respect to the inclusion of the correlation behavior into the inverse Frobenius–Perron problem.

II. GENERAL SOLUTION OF THE IFPP FOR UNIMODAL ERGODIC AND COMPLETE CHAOTIC MAPS

Let us consider the variety of dynamical systems which belong to an arbitrary but fixed invariant density. The solution to this inverse problem is of great interest for the numerical simulation of real physical systems as well as the understanding of the relationship between the functional form of the map and the statistical features of its resulting dynamics. In the present section we establish a general representation of all ergodic and complete chaotic maps of the unit interval (CUM) with a given invariant density and prescribed symmetry. A mere coordinate transformation of an exact map [i.e., a map with constant invariant density $\rho(x)=1$], as described for example in Ref. 19, is of no help to solve this problem. It results in a map with a prescribed invariant measure, but provides no way to control the symmetry properties of the resulting map. Therefore, we choose a different approach and start with a general representation of the solution of the so-called inverse Frobenius–Perron problem (IFPP).[8–13] As a set of solutions of this problem we consider the important class of maps which is only restricted by the requirement of continuity and the property that each branch of the map covers the complete unit interval. These maps are ergodic in the sense that the set of trajectories with positive Liapunov exponent is of measure one. The starting-equation for the construction of the map is the Frobenius–Perron equation:

$$\rho(y)|dy| = \sum_{x_i = f^{-1}(y)} \rho(x_i)|dx_i|, \tag{1}$$

where the summation runs over all preimages of y [for unimodal maps $i = L(left), R(right)$]. For any given unimodal $f(x)$ the right or left preimage of y is determined, once the corresponding other one is given. The essential feature of our approach is the inversion of this expression: A prescribed relation between the two preimages reduces the number of independent differentials on the right-hand side of Eq. (1) and allows the following integration. Such a relation may be described by a function $h_f(x)$, mapping the left preimage onto the right one:

$$h_f : [0, x_{\max}] \to [x_{\max}, 1],$$
$$x_R = h_f(x_L)$$

with

$$f(x_L) = f(x_R), \tag{2}$$

where $x_{\max}$ is the position of the maximum of the unimodal map. $h_f(x)$ is a function monotonously decreasing on the defining interval and it is differentiable with the exception of a finite number of points. It obeys

$$h_f'(x) < 0, \quad x \in [0, x_{\max}],$$
$$h_f(0) = 1, \quad h_f(x_{\max}) = x_{\max}. \tag{3}$$

Substituting h_f in Eq. (1) yields:

$$\rho(y)dy = \rho(x_L)dx_L - \rho(h_f(x_L))h_f'(x_L)dx_L. \tag{4}$$

Using the expression $\mu(x) = \int_0^x \rho(t)dt$ for the invariant measure Eq. (4) can be integrated in $0 < x < x_{\max}$ yielding

$$\int_0^{f_L(x)} \rho(t)dt = \int_0^x [\rho(t) - \rho(h_f(t))h_f'(t)]dt,$$

$$\mu(f_L(x)) = \int_0^x \rho(t)dt - \int_{h_f(0)}^{h_f(x)} \rho(t)dt,$$

$$\mu(f_L(x)) = \mu(x) - \mu(0) - \mu(h_f(x)) + \mu(h_f(0)),$$

where $f_L(x) = f(x)|_{[0,x_{\max}]}$ is the left part of the map $f(x)$. Since we have $h_f(0) = 1$, $\mu(0) = 0$, and $\mu(1) = 1$ we arrive at

$$f_L(x) = \mu^{-1}[\mu(x) - \mu(h_f(x)) + 1] \tag{5}$$

for the left part of the map. The right part of the map, $f_R(x) = f(x)|_{[x_{\max},1]}$, is obtained by substitution of $x \to h_f^{-1}(x)$ in Eq. (5). It follows that the map $f(x)$ parametrized through the function $h_f(x)$ and characterized by the invariant measure $\mu(x)$, is given by

$$f(x) = \left\{ \begin{array}{ll} \mu^{-1}[\mu(x) - \mu(h_f(x)) + 1]; & 0 \leq x < x_{\max} \\ \mu^{-1}[\mu(h_f^{-1}(x)) - \mu(x) + 1]; & x_{\max} \leq x \leq 1 \end{array} \right\}$$
$$= \mu^{-1}(1 - |\mu(x) - \mu(H_f(x))|) \tag{6}$$

where $H_f(x)$ is given by:

$$H_f(x) = \begin{cases} h_f(x), & 0 \leq x < x_{\max} \\ h_f^{-1}(x), & x_{\max} \leq x \leq 1. \end{cases} \tag{7}$$

With the above Eq. (6) we have found an interesting representation and answer to the IFPP which is the central topic of this paper: All CUM with prescribed invariant measure are given by (6), $h_f(x)$ taking on all possible functional forms obeying (2) and (3). This shows that a fixed invariant measure is a relatively weak constraint to a solution of the inverse problem and there is still a considerable freedom to model the mapping.

Before we apply the above approach in order to analyze specific examples (see the following sections) let us demonstrate in the remaining part of this section an alternative way to solve the IFPP. This method is known in the literature[16,17,20,21] as the conjugation transformation approach and has been derived to construct symmetric maps with prescribed invariant measure. We will show (see below) that it is possible to extend this method to generate maps with prescribed invariant measure and any prescribed symmetry properties. This extension can be shown to be closely related to our method utilizing $h_f(x)$. We first briefly review the method of conjugation transformation: Using as a basis the tent map given by: $t(x)=1-|2x-1|$ and applying the conjugation transformations $u(x)$ we obtain $C_1=\{g(x)|g(x)=u^{-1}\circ t\circ u(x)\}$ with $u(0)=0, u(1)=1, u'(x)>0$ for all $x\in[0,1]$ and with the additional property $u(x)=1-u(1-x)$ (antisymmetric with respect to $x_{\max}=\frac{1}{2}$). C_1 is the space of all doubly symmetric maps (symmetric maps and symmetric invariant densities). The invariant density of the transformed map $g(x)$ is then: $\rho_g(x)=|du(x)/dx|$. To arrive in an analogous way at a nonsymmetric density while the map remains symmetric we have to use the transformations $C_2=\{f(x)|f(x)=U^{-1}\circ t\circ u(x)\}$ with $U(x)=u(x)+v(x)$ which are in a sense transverse to conjugation.[20] For symmetric $f(x)$ the function $v(x)$ must also be symmetric: $v(x)=v(1-x)$. The two constraints, i.e., that the invariant density of the resulting map $f(x)$ is a prescribed function $\rho(x)$ and that $f(x)$ is symmetric, determine uniquely $u(x),v(x)$. Defining the symmetric $\mu_+(x)=\frac{1}{2}\int_0^x(\rho(t)-\rho(1-t))dt$ and antisymmetric parts $\mu_-(x)=\frac{1}{2}\int_0^x(\rho(t)+\rho(1-t))dt$ (with $\mu(x)=\mu_+(x)+\mu_-(x)$) of the invariant measure $\mu(x)$ we find: $u(x)=\mu_-(x)$; $v(x)=\mu_+(x)$. Using the fact that: $\mu_-(x)=\frac{1}{2}(\mu(x)+1-\mu(1-x))$ we get the following expression for the desired map $f(x)$:

$$f(x)=\mu^{-1}[1-|\mu(x)-\mu(1-x)|]. \tag{8}$$

Comparing Eqs. (6) and (8) we see that they are compatible provided that $h_f(x)=1-x$, which corresponds to the correct choice of h_f in (6) for a symmetric solution $f(x)$. This clearly demonstrates that in particular the class C_1 but also C_2 represent very special transformations and the class C_2 corresponds only to the special case $h_f(x)=1-x$ within the whole class of maps described by Eq. (6) for a general function h_f.

We now extend the above-described approach, which can be found in the cited references, to arbitrary single humped chaotic and ergodic maps and in particular, in view of the IFPP, to nonsymmetric maps with a given invariant density. For the derivation of Eq. (8) we have used a decomposition of the invariant measure in a symmetric and an antisymmetric part (with respect to $x_{\max}$). This decomposition leads us to a symmetric solution. A general decomposition $\mu_+(x),\mu_-(x)$ obeying $\mu_+(x)+\mu_-(x)=\mu(x)$ is given in the following. In the case of unimodal maps we introduce the following components of the measure $\mu(x)$:

$$\begin{aligned}\mu_+(x)&=\frac{1}{2}\int_0^x(\rho(t)+H_f'(t)\rho(H_f(t)))dt,\\ \mu_-(x)&=\frac{1}{2}\int_0^x(\rho(t)-H_f'(t)\rho(H_f(t)))dt,\end{aligned} \tag{9}$$

with $H_f(x)$ given in Eq. (7). Using the general transformations C_2 with $u(x)=\mu_-(x)$ and $v(x)=\mu_+(x)$ from Eq. (9) we get the solutions given in Eq. (6). Thus the transformations C_2 with $u(x),v(x)$ chosen as in Eq. (9) span the entire space of CUM with a given invariant density $\rho(x)$. They represent therefore a generalization compared to previously defined conjugation transformations or transformations transverse to conjugation.

III. AN EXTENSIVE CLASS OF MAPS WITH THE BETA DISTRIBUTION AS INVARIANT DENSITY

The method to construct a one-dimensional unimodal map with a prescribed invariant density, as proposed in Sec. II, applies for all possible forms of the invariant measure $\mu(x)$ and the invariant density $\rho(x)$, respectively. Nevertheless we want to consider a special class of particularly relevant invariant densities $\rho(x)$, namely the two-parametric beta distribution:

$$\rho(x)=\frac{x^\alpha(1-x)^\beta}{B(\alpha+1,\beta+1)},\quad \alpha,\beta>-1, \tag{10}$$

with the beta function given by

$$B(\alpha+1,\beta+1)=\int_0^1 x^\alpha(1-x)^\beta dx.$$

These densities are important due to their widespread occurrence and applicability (for example in turbulent reacting flows, diffusion in disordered media, image classification see Ref. 22) as well as their simple form. The special case of a symmetric density ($\alpha=\beta$) with a symmetric solution, i.e., a map obeying ($f(x)=f(1-x)$), which is unique, has already been discussed in the literature.[7] We call this solution the doubly symmetric beta map. In the present paper we discuss the general case of an asymmetric invariant density ($\alpha\neq\beta$).

We focus on two solutions of the IFPP with this general asymmetric invariant density, both of which are identical to the doubly symmetric one in the case $\alpha=\beta$:

(1) The first solution is symmetric ($f(x)=f(1-x)$). We call it the symmetric beta map (SB).
(2) The second solution obeys the following constraint:

$$f(x_L)=f(x_R)\quad \text{for } x_L,x_R \text{ with } \rho(x_L)=\rho(x_R), \tag{11}$$

which is only possible if $\alpha\beta>0$. We call this solution the special asymmetric beta map (SAB). In Fig. 1 we show an example of such a map for the case $\alpha=-0.9$, $\beta=-0.6$. The corresponding invariant density is also presented and the notation regarding the imposed constraint of Eq. (11) is explained.

In the following we consider only examples where both α and β possess the same sign, i.e., the above criterion is fulfilled. These two types of solutions correspond of course

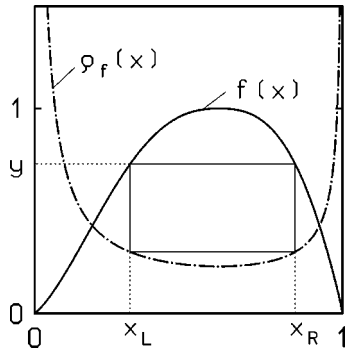

FIG. 1. The SAB map for $\alpha=-0.9$, $\beta=-0.6$, and the corresponding invariant density.

to two different choices for the form of the function $h_f(x)$. For the case of the SB we have $h_f(x)=1-x$. The second case is more delicate. It corresponds to an implicitly defined $h_f(x)$. From the condition in Eqs. (11) and (10) we find:

$$(1-x_R)x_R^{\gamma}=(1-x_L)x_L^{\gamma}, \tag{12}$$

where $\gamma=\alpha/\beta$. Equation (12) defines h_f and can be solved parametrically. Using $\lambda=x_L/x_R$ we get:

$$x_L=\lambda\,\frac{1-\lambda^{\gamma}}{1-\lambda^{\gamma+1}}, \quad x_R=\frac{1-\lambda^{\gamma}}{1-\lambda^{\gamma+1}}, \tag{13}$$

with $0\leqslant\lambda\leqslant 1$. Let us now apply the theoretical considerations of Sec. II to derive the expressions for the two types of beta maps referred to above. The invariant measure corresponding to the density (10) is:

$$\mu_B(x)=\frac{\int_0^x dt\, t^{\alpha}(1-t)^{\beta}}{B(\alpha+1,\beta+1)}=\frac{B(\alpha+1,\beta+1,x)}{B(\alpha+1,\beta+1)}, \tag{14}$$

where $B(a,b,z)$ is the incomplete beta function.[23] Using Eq. (5) we can determine implicitly the left branch of the solution of the IFPP:

$$\begin{aligned}B(\alpha+1,\beta+1,f_L(x))=&B(\alpha+1,\beta+1,x)\\&-B(\alpha+1,\beta+1,h_f(x))\\&+B(\alpha+1,\beta+1)\end{aligned} \tag{15}$$

and a similar expression results also for $f_R(x)$:

$$\begin{aligned}B(\alpha+1,\beta+1,f_R(x))=&B(\alpha+1,\beta+1,h_f^{-1}(x))\\&-B(\alpha+1,\beta+1,x)\\&+B(\alpha+1,\beta+1).\end{aligned} \tag{16}$$

To get the two special solutions referred to above we have to substitute in Eqs. (15) and (16) the suitable h_f. As we already mentioned for the SB we choose $h_f(x)=h_f^{-1}(x)=1-x$. Taking into account this special form of h_f and the fact that Eqs. (15) and (16) are valid for $x<x_{\max}$ and $x>x_{\max}$, respectively (for SB $x_{\max}=\frac{1}{2}$), we can recast Eqs. (15) and (16) into a single equation:

$$\begin{aligned}B(\alpha+1,\beta+1,y_{\mathrm{SB}})=&B(\alpha+1,\beta+1)-\big|B(\alpha+1,\beta+1,x)\\&+B(\beta+1,\alpha+1,x)\\&-B(\alpha+1,\beta+1)\big| \quad x\in[0,1]\end{aligned} \tag{17}$$

with $y_{\mathrm{SB}}=f_{L,\mathrm{SB}}(x)$ for $0\leqslant x\leqslant x_{\max}$ and $y_{\mathrm{SB}}=f_{R,\mathrm{SB}}(x)$ for $x_{\max}<x\leqslant 1$. To calculate the value of the SB for a given x we have to solve Eq. (17) numerically using a standard root finding routine. It turns out that the bisection method[24] is well suited for a fast and accurate determination of y_{SB}. In Fig. 2(a) we present four characteristic members of the class of symmetric beta maps calculated numerically using (17).

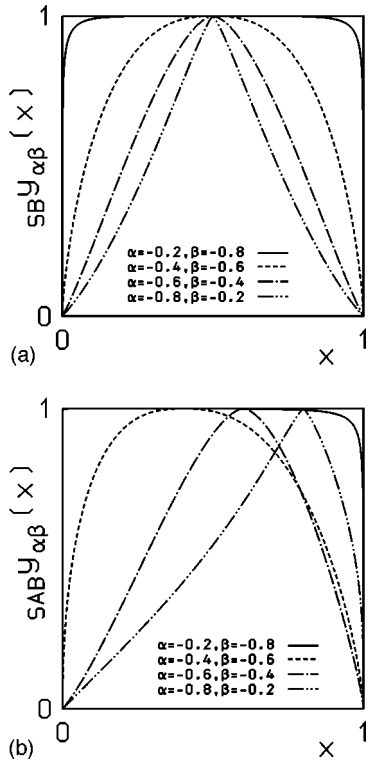

FIG. 2. Characteristic members of the family of maps with the beta distribution as invariant density: (a) Four maps belonging to the SB class. (b) The corresponding four maps of the SAB class.

Let us now return to the SAB case. The calculation of the map y_{SAB} is a little more tedious. For a given x we use Eq. (12) to find numerically $x_R(x_L)$ if $x<x_{\max}$ (if $x>x_{\max}$). Note that for the SAB $x_{\max}=\alpha/(\alpha+\beta)$. The numerical solution to Eq. (12) can be easily obtained using the bisection method. Then we apply Eq. (6) to determine y_{SAB}:

$$B(\alpha+1,\beta+1,y_{\mathrm{SAB}})=\begin{cases}B(\alpha+1,\beta+1,x)-B(\alpha+1,\beta+1,x_R)+B(\alpha+1,\beta+1), & 0\leqslant x<x_{\max}\\ B(\alpha+1,\beta+1,x_L)-B(\alpha+1,\beta+1,x)+B(\alpha+1,\beta+1), & x_{\max}\leqslant x\leqslant 1.\end{cases} \tag{18}$$

Again we have to find the root y_{SAB} of Eq. (18) numerically using the bisection method, since for typical choices of fractional α and β, the inverse beta function is not given explicitly. The calculated SAB maps, for the same choice of the values of α and β as in Fig. 2(a), are presented in Fig. 2(b).

For both types of maps SB and SAB a dynamical route to the fully chaotic and ergodic state can be constructed applying the method described in Ref. 7. Using the numerical solutions to Eqs. (17), (18) we calculated trajectories for the corresponding maps for different values of the parameters α and β. Averaging over a long trajectory of each map we reproduced with a good agreement the invariant densities given as the input for the construction of these maps. We mention that, due to computational accuracy reasons, for α,β values close to -1 it is necessary to calculate $1-y$ instead of y in that range of x for which $y(x)\approx 1$.

Finally let us introduce the concept of the complementary beta map. Two maps $y(x)$ and $\tilde{y}(x)$ belonging to SB or SAB are called complementary, if their invariant densities $\rho(x)$ and $\tilde{\rho}(x)$ are transformed into each other by changing x to $1-x$. Considering the Frobenius–Perron equation, which is the starting point for the construction of both SB and SAB maps, the following relation can be derived:

$$B[\alpha+1,\beta+1,y(x)]=B[\beta+1,\alpha+1,\tilde{y}(1-x)]. \tag{19}$$

Complementary maps agree with respect to certain dynamical features, e.g., the Liapunov exponent, as shown below.

IV. ANALYTICAL AND DYNAMICAL PROPERTIES OF THE SB AND SAB

Many features of the dynamics generated by a discrete map do not depend on the dynamical law as a whole, but only on its local behavior in certain regions of the phase space. In particular, for the case of unimodal maps the order of the maximum turns out to be responsible for some interesting quantities characterizing the underlying dynamics like the singularities of the invariant density at $x=0$ and $x=1$, the decay constant of the autocorrelation, and the scaling parameter of the Feigenbaum bifurcation route.[25] The order ν_m of a map at its maximum $x_{\max}$, is defined as the exponent in the approximation:

$$f(x)\approx 1-|x-x_{\max}|^{\nu_m} \quad \text{for } x\approx x_{\max}. \tag{20}$$

In an analogous way we can define the order of the map at the end points: $x=0,1$. In the following we will determine the corresponding exponents ν_m,ν_0,ν_1 for the SB and SAB.

A. The SB case

One can easily utilize the Frobenius–Perron equation

$$\frac{dy}{dx}=\frac{x^{\alpha}(1-x)^{\beta}+x^{\beta}(1-x)^{\alpha}}{y^{\alpha}(1-y)^{\beta}}, \tag{21}$$

where $y=f(x)$ is the SB map. For $x\to x_{\max}=\frac{1}{2}$, i.e., $y\to 1$, the nominator on the right-hand side of Eq. (21) is finite, which yields $dy/dx\propto 1/[y^{\alpha}(1-y)^{\beta}]$ i.e., $dy/dx(1-y)^{\beta}\propto 1/y^{\alpha}\approx O(1)$ for $y\approx 1$. Assuming $\nu_{m,\mathrm{SB}}$ to be the order of the map in the maximum, i.e. $(1-y)\propto|x-\frac{1}{2}|^{\nu_{m,\mathrm{SB}}}$ and therefore $dy/dx\propto|x-\frac{1}{2}|^{\nu_{m,\mathrm{SB}}-1}$, one gets $|x-\frac{1}{2}|^{\nu_{m,\mathrm{SB}}-1+\beta\nu_{m,\mathrm{SB}}}\approx O(1)$. Since we consider $x\to\frac{1}{2}$ the exponent must vanish, which results in

$$\nu_{m,\mathrm{SB}}=\frac{1}{\beta+1}. \tag{22}$$

Expanding Eq. (17) around the points $x=0$ and $x=1$ and taking into account that $y_{\mathrm{SB}}\to 0$ for $x\to 0$ or $x\to 1$ we find the exponents $\nu_{0,\mathrm{SB}}$ and $\nu_{1,\mathrm{SB}}$ to be:

$$\nu_{0,\mathrm{SB}}=\nu_{1,\mathrm{SB}}=\frac{\min(\alpha,\beta)+1}{\alpha+1}. \tag{23}$$

B. The SAB case

Determining the order of the SAB at its maximum $x_{\max}=\alpha/(\alpha+\beta)$ turns out to be slightly more complicated compared to the case of the SB due to the implicit form of h_f. The derivative dy/dx of the SAB $y=f(x)$ is given by the Frobenius–Perron equation. In terms of the parametric solution $x_R(\lambda),x_L(\lambda)$ of Eq. (13) we get:

$$\frac{dy(x)}{dx}=\begin{cases}\dfrac{dy(\lambda)}{d\lambda}\Big/\dfrac{dx_R}{d\lambda}, & 0<x<x_{\max}\\[2ex] \dfrac{dy(\lambda)}{d\lambda}\Big/\dfrac{dx_L}{d\lambda}, & x_{\max}<x<1\end{cases}. \tag{24}$$

The limit $|x-x_{\max}|\to 0$ corresponds to the limit of Eq. (24) for $\lambda\to 1$. Higher derivatives d^ny/dx^n are obtained by differentiating $d^{n-1}y/dx^{n-1}$ with respect to λ and subsequently dividing by $dx_L/d\lambda$ or $dx_R/d\lambda$, respectively. The leading behavior of the left or right derivative $d^ny/dx^n|_{L,R}$ for $y\to 1$ [which corresponds to $|x-x_{\max}|\to 0$] is given by:

$$\left.\frac{d^ny}{dx^n}\right|_{L,R}\sim\frac{\dfrac{d^ny}{d\lambda^n}}{\left(\dfrac{dx_{L,R}}{d\lambda}\right)^n}. \tag{25}$$

A straightforward but tedious calculation shows that $d^ny/dx^n\propto 1/(1-y)^{n\beta+(n-1)}$. The exponent of $(1-y)$ vanishes for a value

$$n=\nu_{m,\mathrm{SAB}}=\frac{1}{\beta+1}, \tag{26}$$

which gives the order $\nu_{m,\mathrm{SAB}}$ of the SAB at the maximum. Expanding Eq. (18) around the end points $x=0,1$ we get:

$$\nu_{0,\mathrm{SAB}}=\min\left(1,\frac{\alpha(1+\beta)}{\beta(1+\alpha)}\right),\quad \nu_{1,\mathrm{SAB}}=\min\left(\frac{\beta}{\alpha},\frac{1+\beta}{1+\alpha}\right). \tag{27}$$

According to the behavior of the SB and the SAB near the characteristic points 0, 1, $x_{\max}$ we can classify the forms of maps which we obtain for different values of α and β as follows.

(1) *The region* $x\approx x_{\max}$: The order of the map at $x_{\max}$, given by $\nu_m=1/(1+\beta)$, is a common quantity for all beta maps. Maps with $\beta<0$ are differentiable and therefore flat at

$x_{\max}$. With β approaching -1, the maps become increasingly flatter. $\beta>0$ results in a cusp-like shape of the map near $x_{\max}$.

(2) *The zero points 0 and 1:* As far as the form of the maps near the points 1 and 0 is concerned, four limiting cases with certain values for α and β can distinguished.

(a) $\alpha\approx 0, \beta\approx -1$: The maps belonging to both SAB and SB show divergent derivatives $f'(0)\to\infty, f'(1)\to-\infty$. The map itself has a convex shape. As the maximum of the SAB is in $[0, \frac{1}{2}]$, the right branch of the map, containing the unstable fixed point, is more shallow than that of the corresponding SB map.

(b) $\alpha\approx -1, \beta\approx 0$: At $x=0$, both the SB as well as the SAB map develop a slope $f'(0)\to 1$ which enables them to generate intermittent dynamics. Since the SB are symmetric we have $f'(1)\to -1$. The derivatives of the SAB maps however show divergent behavior, $f'(1)\to-\infty$.

The SB and SAB maps are identical to the doubly symmetric one for $\alpha=\beta$. The derivatives of the maps $f'(0)$ and $f'(1)$ take on finite values.

(c) $\alpha=\beta\approx 0$: The limit $\alpha=\beta\to 0$ of the maps is the tent map $f'(0)\to 2, f'(1)\to -2$.

(d) $\alpha=\beta\approx -1$: The values of $f'(0)=-f'(1)$ are still finite, but increase unbounded in the limit $\alpha=\beta\to -1$. The map is extremely flat about the maximum and takes on values very close to 1 in nearly the whole interval [0,1].

The dynamics generated by both the SAB and the SB result in singularities of the invariant density at $x=0,1$ for $-1<\alpha, \beta<0$. Although the strengths of these singularities can be directly read from Eq. (10) it is of interest to explore how they are determined through the order of the map at the maximum and at the end points 0,1. The strength of the singularity at $x=1$ is determined by the order of the maximum only. As the order of the map for both SB and SAB at its maximum is given by $\nu_m=1/(\beta+1)$, the expansion of the map in this region reads

$$1-y\approx|x-x_{\max}|^{\nu_m}=|x-x_{\max}|^{1/(\beta+1)}. \tag{28}$$

Near $x_{\max}$ the invariant measure is a smooth function. Using Eq. (1) we can therefore write $\rho(y)|dy|\propto|dx|$. The dependence of the differential $|dy|$ on x is given by $|dy|\approx[1/(\beta+1)](x-x_{\max})^{1/(\beta+1)-1}|dx|$. If we now make the ansatz $\rho(y)\propto(1-y)^{\tilde\beta}$ for the invariant density at $x\approx 1$, the Frobenius–Perron equation in orders of x reads

$$|x-x_{\max}|^{\tilde\beta[1/(\beta+1)]}|x-x_{\max}|^{1/(\beta+1)-1}|dx|$$
$$\propto|dx|\Rightarrow\tilde\beta\frac{1}{\beta+1}+\frac{1}{\beta+1}-1=0\Rightarrow\tilde\beta=\beta. \tag{29}$$

We therefore conclude that the strength of the singularity of the invariant density at $x=1$ for both types of maps (SB and SAB) is given implicitly by the order of the dynamic law at its maximum.

The determination of the singularity at $x=0$ is more intricate. We will study in detail the case of the SB maps. The SAB maps can be treated in an analogous way. For the SB family the Frobenius–Perron equation can be written in the form:

$$\rho(y_{\rm SB})|dy_{\rm SB}|=[\rho(x)+\rho(1-x)]|dx|, \tag{30}$$

Using Eq. (23) the SB at $x\approx 0$ is approximately given by $y_{\rm SB}\approx x^{[\min(\alpha,\beta)+1]/(\alpha+1)}$. Let us make the ansatz $\rho(y_{\rm SB})\propto y_{\rm SB}^{\tilde\alpha}$ for the singularity of the invariant density at $y_{\rm SB}=0$. For $x\approx 0$ $\rho(x)$ and $\rho(1-x)$ possess the singularities $\tilde\alpha$ and β, respectively. Therefore the Frobenius–Perron equation reads

$$x^{\tilde\alpha[\min(\alpha,\beta)+1]/(\alpha+1)}x^{[\min(\alpha,\beta)+1]/(\alpha+1)-1}|dx|\propto x^{\min(\tilde\alpha,\beta)}|dx| \tag{31}$$

$$\Rightarrow\tilde\alpha\frac{\min(\alpha,\beta)+1}{\alpha+1}+\frac{\min(\alpha,\beta)+1}{\alpha+1}-1=\min(\tilde\alpha,\beta). \tag{32}$$

Two cases have to be considered.

(1) The first possibility is $\min(\alpha,\beta)=\beta$. In this case Eq. (32) yields $\tilde\alpha(\beta+1)+(\beta-\alpha)=(\alpha+1)\min(\tilde\alpha,\beta)$ and therefore

$$\min(\tilde\alpha,\beta)=\frac{\beta(\tilde\alpha+1)+(\tilde\alpha-\alpha)}{\alpha+1} \tag{33}$$

with the solution $\alpha=\tilde\alpha$. The singularity at $x=0$ is given by the parameter α as expected.

(2) The case $\alpha<\beta$ demands slightly more attention. The order of the map in $x=0$ and $x=1$ is one, according to Eq. (23). This makes the dynamics a candidate for intermittency, which has already been the subject of many investigations.[26–28] It is characterized by an expansion of the map near a marginally unstable fixed point of the form

$$y(x)\approx x+\epsilon x^z,\quad x\to 0. \tag{34}$$

The order of the next-to-leading term, z, determines essentially the statistical properties of the dynamical law near $x=0$. In Ref. 15 it is shown, that a symmetric map, with a maximum of order ν_m and of the form (34) at $x=0$, generates an invariant density, which has a singularity of the order

$$\tilde\alpha=\frac{1}{\nu_m}-z \tag{35}$$

at $x=0$. Using the implicit representation of the SB map:

$$B(\alpha+1,\beta+1,y_{\rm SB})=B(\alpha+1,\beta+1,x)$$
$$+B(\beta+1,\alpha+1,x),\quad x<\tfrac{1}{2} \tag{36}$$

and expanding the incomplete beta functions about $x=0$ with the help of the formula:

$$B(\alpha+1,\beta+1,t)\approx\frac{t^{\alpha+1}}{\alpha+1}-\beta\frac{t^{\alpha+2}}{\alpha+2} \tag{37}$$

we find:

$$\frac{y_{\rm SB}^{\alpha+1}}{\alpha+1}\approx\frac{x^{\alpha+1}}{\alpha+1}+\frac{x^{\beta+1}}{\beta+1}. \tag{38}$$

It follows that:

$$y_{\rm SB}\approx x\left(1+\frac{\alpha+1}{\beta+1}x^{\beta-\alpha}\right)^{1/(\alpha+1)}\approx x+\frac{1}{\beta+1}x^{\beta-\alpha+1}. \tag{39}$$

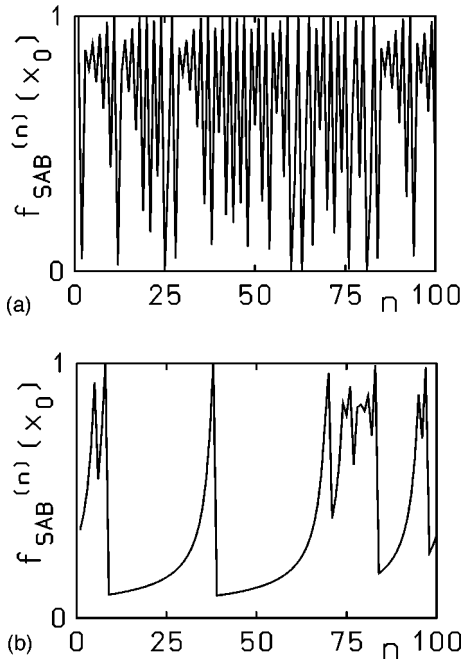

FIG. 3. Characteristic time series, generated by SAB maps: (a) oscillating regime ($\alpha=-0.4, \beta=-0.7$), (b) intermittent regime ($\alpha=-0.8, \beta=-0.1$).

Therefore the term next to the leading one is of order $z=\beta-\alpha+1$. Using Eq. (35) and $\nu_m=1/(\beta+1)$ we find $\tilde{\alpha}=\beta+1-(\beta-\alpha+1)=\alpha$, i.e., the correct strength of the singularity at $x=0$ is reproduced.

At the end of this section let us discuss the different kinds of dynamics which are generated by the different types of maps in the two classes SAB and SB. Depending on the values of α and β, there are two eye-catching types of dynamical behavior.

(1) $0>\alpha>\beta$: The trajectories of both SB and SAB maps are characterized by an oscillatory motion around the unstable fixed point in the right interval of monotony of the map: The critical point $x_{\max}$ of the SAB maps approaches $x=0$. Therefore a relatively large part of the map right of $x_{\max}$ describes a flat curve, with only small curvature and derivative $dy/dx\approx-1$ near the unstable fixed point. These features generate a trajectory oscillating about the unstable fixed point[17] for a considerably long time with exponentially increasing amplitude and highly correlated phase [see Fig. 3(a) for an example]. These characteristics are less pronounced for SB maps with $x_{\max}=\frac{1}{2}$. After leaving this regime we encounter an oscillatory motion of the orbit about the maximum. In this case the left and the right branches of the map are visited alternately. As the parts of the map visited are nearly symmetric with respect to the axis $y(x)=x$, a nearly stable orbit with period two occurs. This peculiar feature of the map is more common for the SB maps. The two singularities of the invariant density are built up by these oscillations. As the center of the oscillations is shifted to the right of $\frac{1}{2}$, the singularity at $x=1$ is stronger than the one at $x=0$.

(2) $\alpha<\beta<0$: The dynamics developed by both the SB and the SAB maps is dominated by the intermittent behavior near the marginally unstable fixed point $x=0$. The trajectories show an interplay of chaotic motion and laminar phases in the region of $x\approx0$. An example for a trajectory is given in Fig. 3(b). The comparison of the maps belonging to the two classes shows nicely the detailed balance of the system generating the same invariant density: For a SAB the exponent z in the expansion $y(\epsilon)\approx\epsilon+\epsilon^z$, $\epsilon\ll1$ is much closer to 1 than for the corresponding SB map and the region of the map where this expansion holds is larger. Therefore the orbit tends to be captured for a longer time in this region. However, due to the diverging derivative of the SAB map at $x=1$, the laminar region is visited less often, which partially compensates the above effect.

V. LIAPUNOV EXPONENTS, AUTOCORRELATIONS, AND POWER SPECTRA FOR SB AND SAB

In this section we derive some dynamical and statistical properties of characteristic members of the SB and SAB classes of maps. First we consider the Liapunov exponents which are a measure for the degree of chaoticity. As the derivatives of both classes SB and SAB are obtained from the Frobenius–Perron equation, the Liapunov exponents $\Lambda^{\mathrm{SB}}_{\alpha,\beta}$ and $\Lambda^{\mathrm{SAB}}_{\alpha,\beta}$, respectively, can be calculated using the definition

$$\Lambda=\int_0^1\rho(x)\ln\left|\frac{dy(x)}{dx}\right|dx.$$

The implicit form of $y(x)$ prevents an analytical treatment. Therefore we have calculated $\Lambda^{\mathrm{SB}}_{\alpha,\beta}$ and $\Lambda^{\mathrm{SAB}}_{\alpha,\beta}$ numerically for different values of $-1<\alpha,\beta<0$, using Eqs. (17) and (18), respectively. Both Liapunov exponents show similar features as functions of α and β. Most striking is the symmetry

$$\Lambda^{\mathrm{SB}}_{\alpha,\beta}=\Lambda^{\mathrm{SB}}_{\beta,\alpha},\quad \Lambda^{\mathrm{SAB}}_{\alpha,\beta}=\Lambda^{\mathrm{SAB}}_{\beta,\alpha}, \tag{40}$$

i.e., the Liapunov exponent stays the same when switching from beta maps to the complementary ones given in Eq. (19). This symmetry is even more astonishing, since it connects two very different kinds of dynamics with the same Liapunov exponent, i.e., with the same degree of chaoticity. The value of the Liapunov exponent is maximal ($\ln 2$) for the doubly symmetric case $\alpha=\beta$ and decreases as $|\alpha-\beta|$ increases. This can be at best seen in Fig. 4 where we show the Liapunov exponent $\Lambda^{\mathrm{SAB}}_{\alpha,\beta}$ as a function of the parameters α,β. The decrease in the degree of chaoticity for the case $\alpha<\beta$ is caused by the frequent occurrence of almost regular intermittent intervals while in the case $\alpha>\beta$ it is caused by the dominating hopping of the orbit around the unstable fixed point of the map.

Let us now turn to the calculation of the autocorrelation function $C(n)$ for the SB and SAB members. When considering data obtained from numerical simulations, one has to consider the finite round-off error. It results in fluctuations of $C(n)$ appearing after a certain number of time steps. This number is independent of the length of the trajectory used to calculate $C(n)$ and limits the reliable range of the correlation functions and power spectra shown in Figs. 5(a) and 5(b), 6(a) and 6(b), 7(a) and 7(b).

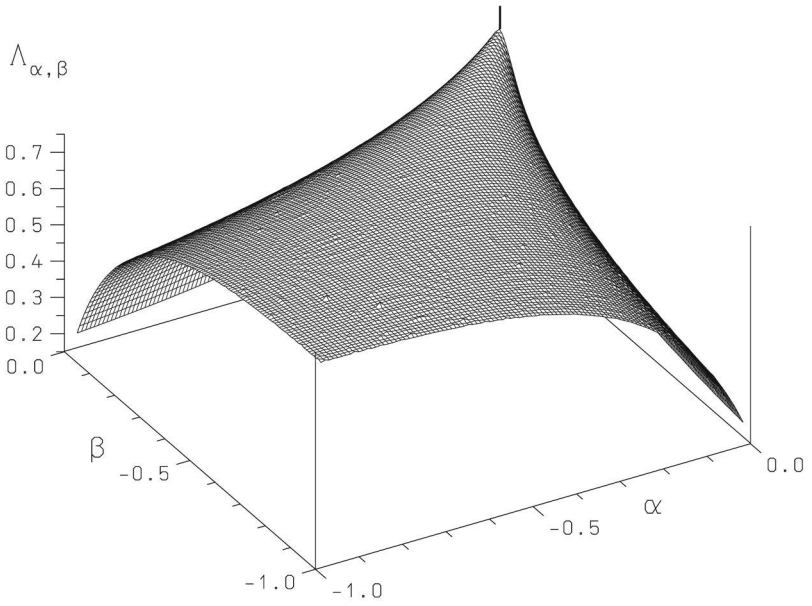

FIG. 4. The Liapunov exponent $\Lambda_{\alpha,\beta}$ for the SAB class as a function of α,β.

Again two types of maps in the SB and SAB classes have to be distinguished.

(1) $\alpha>\beta$: The correlation function is oscillating with period two and decays exponentially fast. This is a consequence of the oscillatory motion of the orbit about the unstable fixed point. The decay of the envelope is slower for maps with $|\beta-\alpha|$ large, since the corresponding map has a more shallow slope of the right interval of monotony, which allows long lasting oscillations. The mean decay time of the SB maps [see Fig. 5(a)] is much shorter compared to those of the SAB maps [see Fig. 5(b)], since the symmetry of the map restricts the length of the highly correlated, oscillating phases of the orbit. Due to this fast decay only a few steps of the correlation function of the SB maps are numerically obtainable.

(2) $\alpha<\beta$: The intermittent dynamics results in a correlation function which decays algebraically in the long time regime according to $C(n)\propto n^{-\eta}$. For weak intermittent dy-

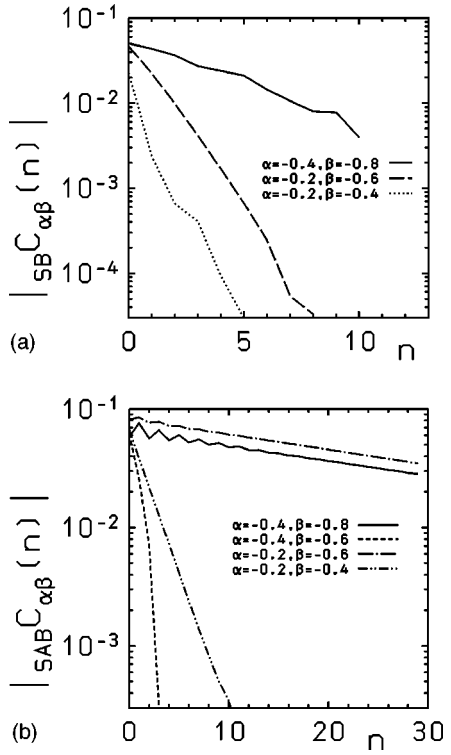

FIG. 5. The absolute value of the autocorrelation function $C_{\alpha,\beta}(n)$ for different values of α,β and in the regime $\alpha>\beta$ (oscillating regime): (a) for SB maps, (b) for maps belonging to the SAB class. The remaining oscillations in (b) show a transient behavior of $C(n)$ for small n.

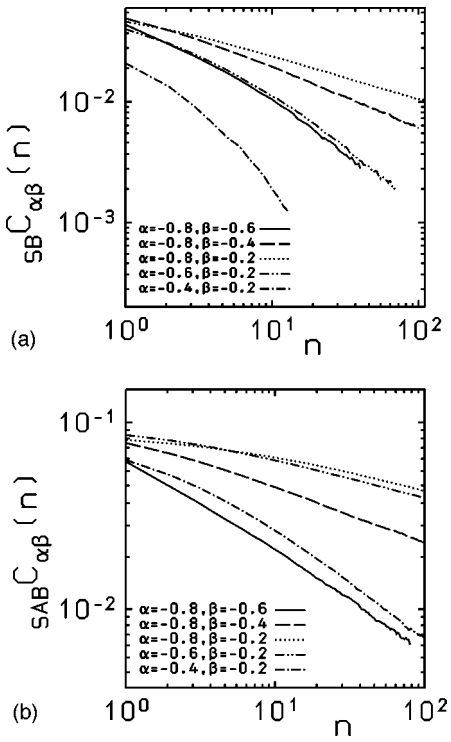

FIG. 6. The autocorrelation function $C_{\alpha,\beta}(n)$ for different values of α,β and for $\alpha<\beta$ (intermittent regime): (a) for SB maps, (b) for maps belonging to the SAB class.

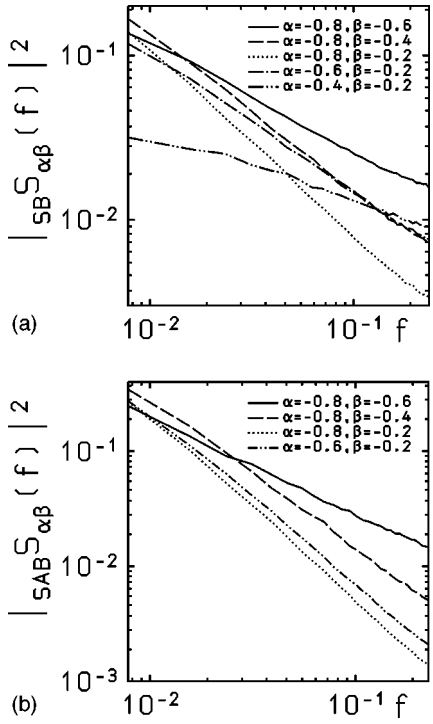

FIG. 7. The square of the absolute value of the power spectrum $S(n)$ for different values of α,β and for $\alpha<\beta$ (intermittent regime): (a) for SB maps, (b) for maps belonging to the SAB class.

namics the decay exponent η can be estimated analytically. For this aim we use the map:

$$y(\epsilon)=\epsilon+a\epsilon^z+\cdots, \quad 0<\epsilon\ll 1. \tag{41}$$

Assuming that the invariant density $\rho(x)$ near the center of intermittency is given by $\rho(\epsilon)\propto\epsilon^\alpha$, $0<\epsilon\ll 1$, $-1<\alpha$, $1<z$ and following Ref. 15 we derive the following scaling relation describing the autocorrelation function in the limit of distinctive intermittent behavior, i.e., $0<z-1\ll 1$ and for $n\to\infty$:

$$C(n)\approx K\left(1+\frac{n}{n_0}\right)^{-\eta} \tag{42}$$

with

$$z=\beta-\alpha+1(\text{SB map}), \quad \eta=\frac{1+\alpha}{z-1}>0,$$
$$\frac{1}{n_0}=(z-1)a(\bar{x}+1)^{z-1}, \tag{43}$$

where K is a constant characteristic for the system. This behavior takes account of the long and highly correlated laminar sections of the orbit. The characteristic exponent η decreases with increasing $|\beta-\alpha|$ and thus corresponds to a slower decay of the correlation. For shorter times a transient behavior leading into the algebraic decay can be seen. The correlation of systems generated by SB maps [Fig. 6(a)] decay faster compared to those SAB maps with the same values for α and β [Fig. 6(b)]. The knowledge of the order of the SB maps in the maximum point and the zeros at $x=0$ and $x=1$ allows a comparison of the characteristic exponent η_{num} obtained numerically with the value η_{cta} obtained by the continuous time approximation in Ref. 15. Results are presented in Table I and show a fair agreement of η_{cta} and η_{num}.

TABLE I. Decay constants of the correlation functions of the intermittent SB maps shown in Fig. 6(a): η_{cta} obtained by continuous time approximation, η_{num} resulting from numerical simulation. The discrepancy between η_{num} and η_{cta} corresponding to $\alpha=-0.4$, $\beta=-0.2$ is probably due to the limited range of the correlation function obtainable for these parameters.

α	β	z	η_{cta}	η_{num}
−0.8	−0.6	1.2	1.00	0.93
−0.4	−0.2	1.2	3.00	1.70
−0.8	−0.4	1.4	0.50	0.56
−0.6	−0.2	1.4	1.00	0.99
−0.8	−0.2	1.6	0.33	0.36

The corresponding power spectrum $S(f)$ of both the SB and SAB maps shows the typical power-law scaling behavior, which is illustrated in Figs. 7(a) and 7(b) for different sets of α,β.

VI. CONCLUSIONS

We have presented a general solution to the inverse Frobenius–Perron problem for a broad class of one-dimensional unimodal complete chaotic maps of the unit interval. This solution allows us to cover a larger than previously considered space of fully chaotic unimodal maps with given invariant density. It is shown that the general solution can also be obtained by a suitably defined transformation. Using this general representation one can find infinitely many particular solutions. To illustrate our method we applied it to obtain two classes of dynamical systems possessing the two parametric beta-probability function as the invariant density. We calculated the Liapunov exponents, autocorrelation functions and power spectra for these maps and studied the properties of the obtained solutions in a twofold manner: First we observed for given values of the parameters of the invariant density the changes in the dynamical and statistical properties for systems corresponding to different partial solutions of the Frobenius–Perron equation. We then varied the parameters of the invariant density remaining within a certain class of partial solutions. From our studies we conclude that two typical properties dominate the dynamics for unimodal beta maps. The first property is the hopping of the chaotic trajectory around the unstable fixed point of the map which leads to an exponential decay of correlations. The decay constant depends on the explicit form of the special solution for given parameters of the invariant density. The second possibility is the intermittent scenario: the chaotic trajectory possesses extended laminar phases in the neighbourhood of $x=0$. The correlations in this case decay with a power law. Theoretical investigations predict that the characteristic exponent in this power-law decay is determined through the singularities of the invariant density at the center of intermittency ($x=0$) as well as the derivative of the map at this point. We tested these estimations and found a satisfactory agreement with our numerical calculations.

Thus our approach to the inverse Frobenius–Perron problem allows us to determine one-dimensional maps with a rich variety of dynamical behavior and enables us to perform accurate calculations for physical observables even in the case where the ergodic limit is computationally inaccessible (intermittency). The obtained general solution involves the function h_f and one might therefore use this degree of freedom to design dynamical laws with more prescribed quantities than the invariant density. One step in this direction would be to solve the inverse Frobenius–Perron problem with the additional constraint of a given autocorrelation function. Using the parameterization (6) of the general solution to the Frobenius–Perron equation it should be in principle possible to design a map which is closest to a certain given correlation behavior. A detailed investigation of this problem is in progress.[29]

ACKNOWLEDGMENTS

F.K.D. gratefully acknowledges financial support from the European Union. P.S. thanks the Max-Planck Institute for Physics of Complex Systems for its kind hospitality.

[1] M. J. Feigenbaum, J. Stat. Phys. **19**, 25 (1978); **21**, 669 (1979).
[2] J. P. Crutchfield, J. D. Farmer, and B. A. Huberman, Phys. Rep. **92**, 45 (1982).
[3] P. Manneville and Y. Pomeau, Phys. Lett. **75A**, 1 (1979); Physica D **10**, 219 (1980).
[4] T. Geisel and J. Nierwetberg, Phys. Rev. Lett. **48**, 7 (1982); Phys. Rev. A **29**, 2305 (1984).
[5] J. E. Hirsch, B. A. Huberman, and D. J. Scalapino, Phys. Rev. A **25**, 519 (1981).
[6] T. Geisel, A. Zacherl, and G. Radons, Phys. Rev. Lett. **59**, 2503 (1987).
[7] F. K. Diakonos and P. Schmelcher, Phys. Lett. A **211**, 199 (1996).
[8] A. Baranovsky and D. Daems, Int. J. Bifurcation Chaos Appl. Sci. Eng. **5**, 1585 (1995).
[9] S. Koga, Prog. Theor. Phys. **86**, 991 (1991).
[10] D. Ghikas, Lett. Math. Phys. **7**, 91 (1983).
[11] C. C. Grosjean, J. Math. Phys. **28**, 1265 (1987).
[12] G. Paladin and S. Vaienti, J. Math. Phys. **21**, 4609 (1988).
[13] F. Y. Hunt and W. M. Miller, J. Stat. Phys. **66**, 535 (1992).
[14] C. Beck, Physica D **41**, 67 (1990).
[15] S. Grossmann and H. Horner, Z. Phys. B **60**, 79 (1985).
[16] S. Grossmann and S. Thomae, Z. Naturforsch. A **32**, 1353 (1977).
[17] H. Mori, B. So, and T. Ose, Prog. Theor. Phys. **66**, 1266 (1981).
[18] H. G. Schuster, *Deterministic Chaos* (VCH Weinheim, 1995).
[19] A. Lasota and M. C. Mackey, *Chaos, Fractals, and Noise* (Springer, New York, 1994).
[20] G. Gyorgyi and P. Szepfalusy, Z. Phys. B **55**, 179 (1983).
[21] A. Csordas, G. Gyorgyi, P. Szepfalusy, and T. Tel, Chaos **3**, 31 (1993).
[22] C. P. Lowe, P. Frenkel, and M. A. van der Foef, J. Stat. Phys. **87**, 1229 (1997); S. S. Girimaji, Phys. Fluids A **4**, 2875 (1992); **4**, 2529 (1992); R. L. Gaffney, Jr., J. A. White, S. S. Girimaji, and J. P. Drummond, ''Modeling temperature and species fluctuations in turbulent reacting flows,'' Comp. Sys. Eng. **5**, 117–133 (1994); E. R. Weeks, J. S. Urbach, and H. L. Swinney, Physica D **97**, 291 (1996); K. Arai, Y. Terayama, and T. Arata, Proc. IEEE **2**, 1263 (1995).
[23] I. S. Gradshteyn and I. M. Ryzhik, *Tables of Series, Products and Integrals* (Academic, New York, 1994).
[24] W. H. Press, B. P. Flannery, S. A. Teukolsky, and W. T. Vetterling, *Numerical Recipes* (Cambridge University Press, Cambridge, 1992).
[25] E. Ott, *Chaos in Dynamical Systems* (Cambridge University Press, Cambridge, 1993).
[26] Z. Kaufmann, H. Lustfeld, and J. Bene, Phys. Rev. E **53**, 1416 (1996).
[27] H. Lustfeld, J. Bene, and Z. Kaufmann, J. Stat. Phys. **83**, 1199 (1996).
[28] J. Bene, Z. Kaufmann, and H. Lustfeld, J. Stat. Phys. **89**, 605 (1997).
[29] F. K. Diakonos and P. Schmelcher (unpublished).